Journal of Alloys and Compounds 508 (2010) 480–485

Contents lists available at ScienceDirect

Journal of Alloys and Compounds

journal homepage: www.elsevier.com/locate/jallcom

Effect of Nd on microstructure and wear resistance of hypereutectic Al–20%Si alloy

W.X. Shi, B. Gao*, G.F. Tu, S.W. Li

School of Materials and Metallurgy, Northeastern University, Shenyang, Liaoning Province 110004, China

ARTICLE INFO

Article history:
Received 8 April 2010
Received in revised form 19 August 2010
Accepted 24 August 2010
Available online 21 September 2010

Keywords:
Hypereutectic Al–Si alloys
Neodymium
Modification
Primary silicon
Wear

ABSTRACT

In this paper, pure Nd was adopted to modify hypereutectic aluminum–silicon alloy (Al–20%Si). The morphology of eutectic and primary silicon phases was analyzed by OM and SEM. OM and SEM results show that pure Nd (0.3 wt.%) can significantly refine both eutectic and primary silicon of hypereutectic Al–20%Si alloy. Morphology of primary silicon was transformed from star-shaped and irregular morphology to fine polyhedral and grain size of primary silicon was refined from 80–120 μm to 20–50 μm. TEM results show that a new needle shape ternary phase ($AlSi_xNd_y$) forms in modified alloy. XRD results show that three little unknown diffraction peaks appear after Nd modification and it is induced that they should be diffraction peaks of ternary $AlSi_xNd_y$ intermetallic phase in the modified alloy by analyzing both TEM and XRD results. Friction and wear resistance tests show that friction coefficient of Al–20%Si alloy decreases after Nd modification. Wear resistance of Al–20%Si alloy after 0.3 wt.%Nd modification was significantly improved as compared to the initial sample. The improvement of wear resistance was mainly attributed to change of morphology, size and distribution of eutectic silicon and primary silicon after Nd modification. The dominant wear mechanism for 0.3 wt.%Nd modified alloy was abrasive wear, adhesive wear and oxidative wear mechanism, but wear mechanism for unmodified alloy was abrasive wear and adhesive wear mechanism.

1. Introduction

Hypereutectic Al–Si alloys are very promising material for aluminum alloys due to their excellent properties, including low coefficient of thermal expansion, low density, good corrosion resistance, high wear resistance, and so on [1–13]. However, with the silicon content increasing, the massive primary silicon and long needle-like eutectic silicon in hypereutectic Al–Si alloys split the matrix and reduce the alloys' performances. So, it is essential for us to modify hypereutectic Al–Si alloys to change morphology and distribution of primary and eutectic silicon phases with an aim of enhancing mechanical properties of the alloys [14–16].

Refinement of primary silicon is usually obtained by the addition of phosphor or phosphorous compounds to the melt. The use of phosphor addition to modify primary silicon in hypereutectic Al–Si alloys has been traced back to a patent by Sterner Rainer [17]. Liu et al. [18] have reported that Al–P master alloy was adopted to refine Al–30%Si alloy with a new refining method, the average size of primary Si is decreased to 30 μm. In the past decades, it was reported that the rare earth (RE) elements were capable of modifying the eutectic structure of cast Al–Si alloys. Chang et al. [19] have reported that simultaneous refinement of both primary silicon (approximately 35 μm, at cooling rate of 45 °C/s) and eutectic silicon was achieved with the addition of misch metal to hypereutectic Al–21 wt.%Si alloy. Yi and Zhang [20] have reported that La could cause modification of eutectic silicon in hypereutectic Al–Si alloys and some of La-rich phase could be observed to envelop some small polygonal silicon crystals.

The wear resistance of cast Al–Si alloys depends on the hardness of the matrix and the dispersed second phase Si particles/plates in matrix [21]. The distribution state of Si particles in the Al–Si alloys can be changed by modification [14–16]. The applications of hypereutectic Al–Si alloys for the machine parts are increasing in the industry. However, little has been reported on the wear behavior of hypereutectic Al–Si alloys with the addition of RE grain refiner and modifier [22–24]. In present study, pure Nd was adopted to modify hypereutectic Al–20%Si alloy with an aim of investigating the effect of pure Nd on microstructure and wear resistance of hypereutectic Al–20%Si alloy. By observation and analysis of worn surfaces, the wear mechanism of the alloys has been investigated.

2. Experimental

2.1. Materials

The chemical compositions of the experimental alloy are shown in Table 1 (all compositions in this work quoted are in (mass fraction (%)).

* Corresponding author. Tel.: +86 24 83681320.
E-mail address: surfgao@yahoo.com.cn (B. Gao).

0925-8388/$ – see front matter © 2010 Elsevier B.V. All rights reserved.
doi:10.1016/j.jallcom.2010.08.098

Table 1
Chemical composition of Al–20%Si alloys (%, mass fraction).

Alloy	Al	Si	RE
Base alloy	Bal.	20	0.0
Modified alloy	Bal.	20	0.3

Table 2
Raw materials specification.

Raw material	Purity (%)	Production place
Al	99.7	Fushun, China
Si	99.99	Yunnan, China
Nd	99.5	Baotou, China

The hypereutectic Al–20%Si alloy used in the experiments was produced by an electrical resistance finance using commercial purity aluminum and commercial purity silicon and modifier was purity Nd. Raw materials specification are shown in Table 2.

2.2. Experimental methods

The hypereutectic Al–Si alloy used in the experiment was melted in electrical resistance finance. Rare earth element Nd was added into alloy at 750–800 °C and held for 10 min at 780 °C. The alloy was poured into an iron mould with length of 150 mm and inner diameter of 15 mm. The modified ingot was obtained. The unmodified ingot was obtained under the same procedure without adding Nd.

Metallographic specimens were line-cut from the ingots and mechanically grounded and polished. The microstructure evolutions were investigated by means of scanning electron microscope (SEM, SSX-550 fitted with EDS equipment) analyses and the samples surface were etched by 0.5% HF before SEM observation. Phase analysis of samples before and after modification was conducted by means of X-ray diffraction (XRD, PW 3040/60). Transmission electron microscopy (TEM, G20 fitted with EDS equipment) was adopted to analyze the microstructure of modified samples with 0.3 wt.%Nd. Energy-dispersive spectroscopy (EDS) was used to analyze the chemical composition of the phases appearing in the TEM observation field. TEM samples were prepared according to the standard process.

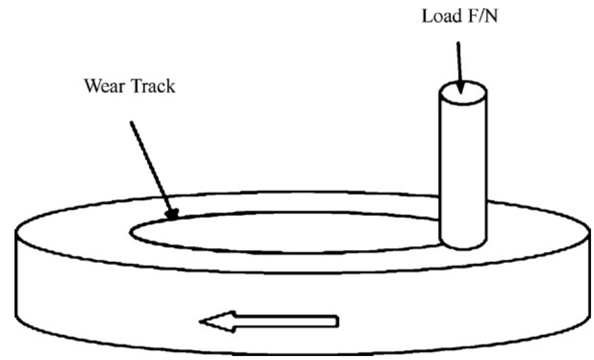

Fig. 1. Principle diagram of pin-on disc wear monitor.

Wear tests were carried out using a MG-2000 type pin-on disc machine with intelligent control system of Vi software (Lab6.1 version). The pin specimens were machined in the form of cylinders with 6 mm diameter and 12 mm length. The counterpart discs were made of stainless steel (1Cr18Ni9) with surface hardness of 192 HV and surface roughness of $R_a = 1\ \mu m$. The applied load was 10 N, 20 N and 30 N. Sliding speed and distance were kept constant at 0.8 m/s and 0.5 km. Principle diagram is shown in Fig. 1.

The weight loss during wear test was measured using an electronic balance with the resolution of ±0.1 mg. Four pins were used during each test. The standard deviation for the weight loss lies in the range of ±10%. The samples were thoroughly cleaned with acetone in ultrasonic cleaner with before and after the wear test. Wear rate was calculated from weight loss and sliding distance. Wear surface of pins was characterized using the SSX-550 type scanning electron microscope (SEM) attached with energy-dispersive spectroscopy (EDS).

3. Results and discussion

3.1. Microstructure

Fig. 2 shows the microstructure characteristic of silicon of unmodified and modified Al–20%Si alloys. Fig. 2(a) is an optical

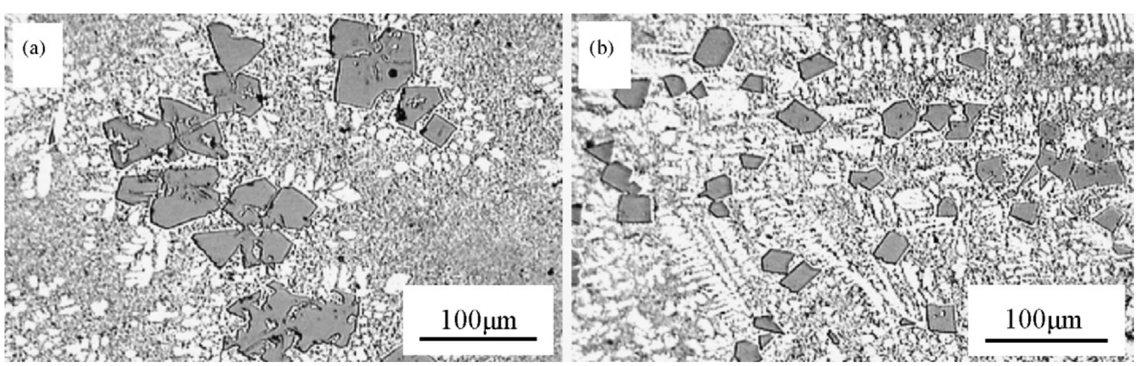

Fig. 2. Microstructure characteristic of silicon of unmodified and modified Al–20%Si alloys. (a) Unmodified sample and (b) modified sample.

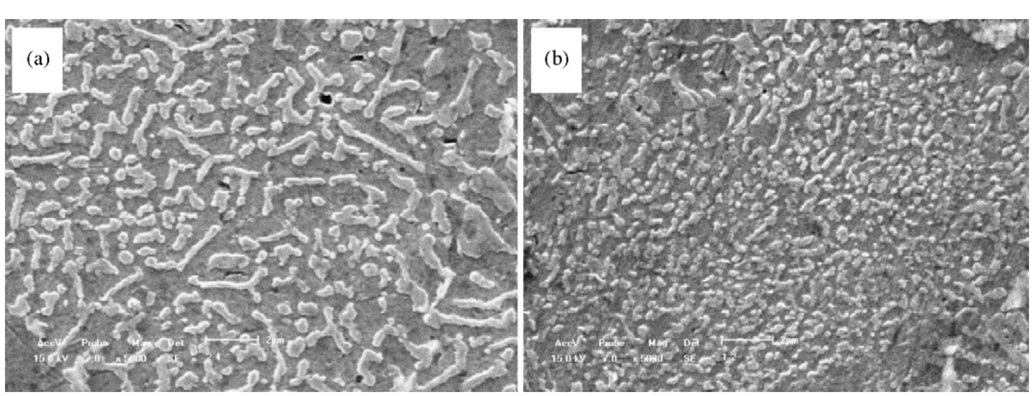

Fig. 3. SEM micrographs of eutectic silicon of Al–20%Si alloy before and after modification. (a) Unmodified sample and (b) modified sample.

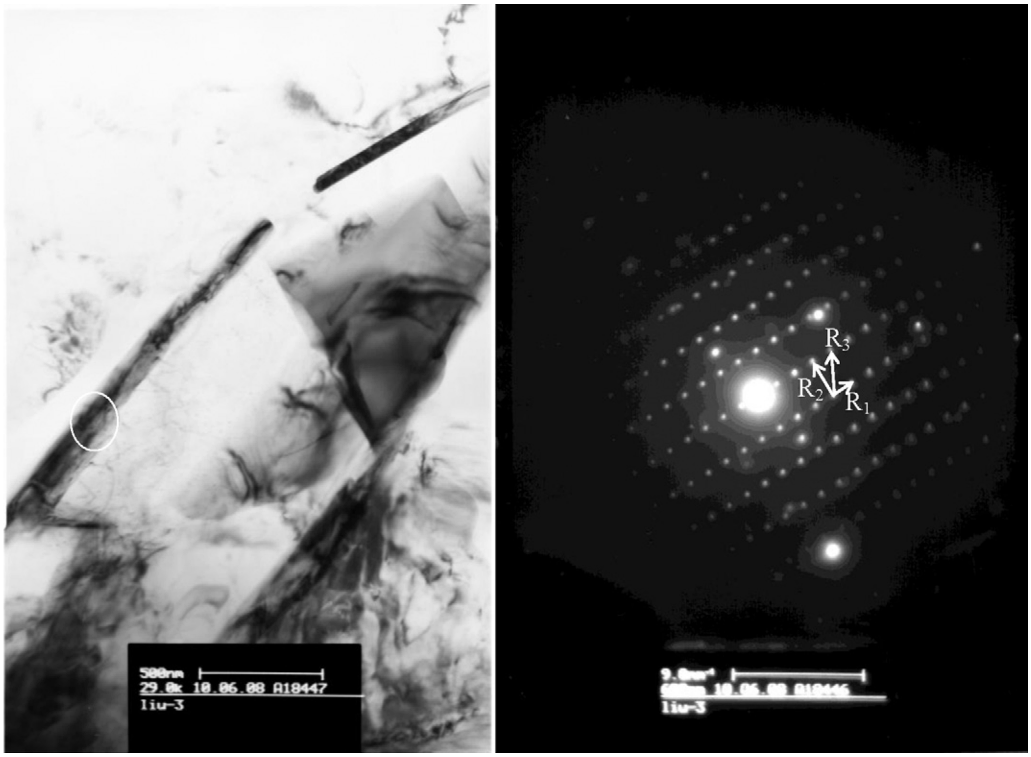

Fig. 4. TEM image and SAD pattern of Al–20%Si–0.3%Nd alloys.

micrograph of unmodified sample after etching. The primary silicon phase shows typical star-shaped and irregular morphology, it is very coarse and the size of the phase even exceeds 120 μm. Fig. 2(b) gives an optical micrograph of sample modified by 0.3 wt.%Nd. The morphology of primary silicon changes from star-shaped and irregular morphology to fine polyhedral, the size of primary silicon is decreased to 20–50 μm. Meantime, the primary silicon in modified sample tends to dispersive distribution as compared to initial sample. It shows that Nd could modify primary silicon significantly.

Fig. 3(a) and (b) present SEM micrographs of eutectic silicon of Al–20%Si alloy before and after modification. Fig. 3(a) gives SEM micrographs of unmodified eutectic silicon of Al–20%Si alloy. The eutectic Si morphology of Al–20%Si alloy is acicular or lamellar. Fig. 3(b) shows eutectic Si morphology of Al–20%Si–0.3%Nd alloy, it can be seen that eutectic silicon morphology changes from acicular

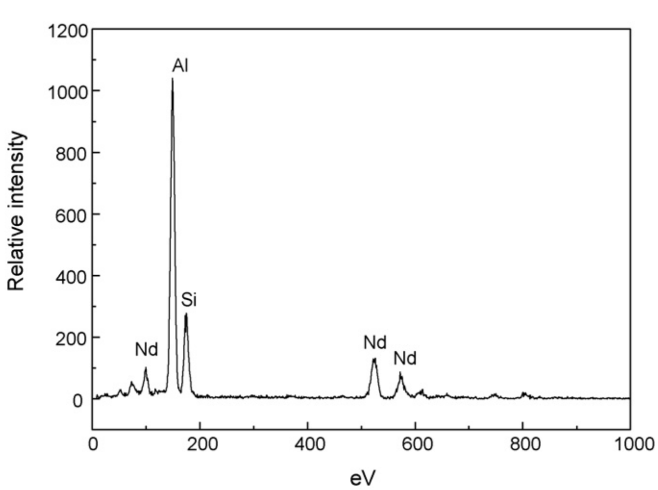

Fig. 5. EDS composition analysis of needle shape phase.

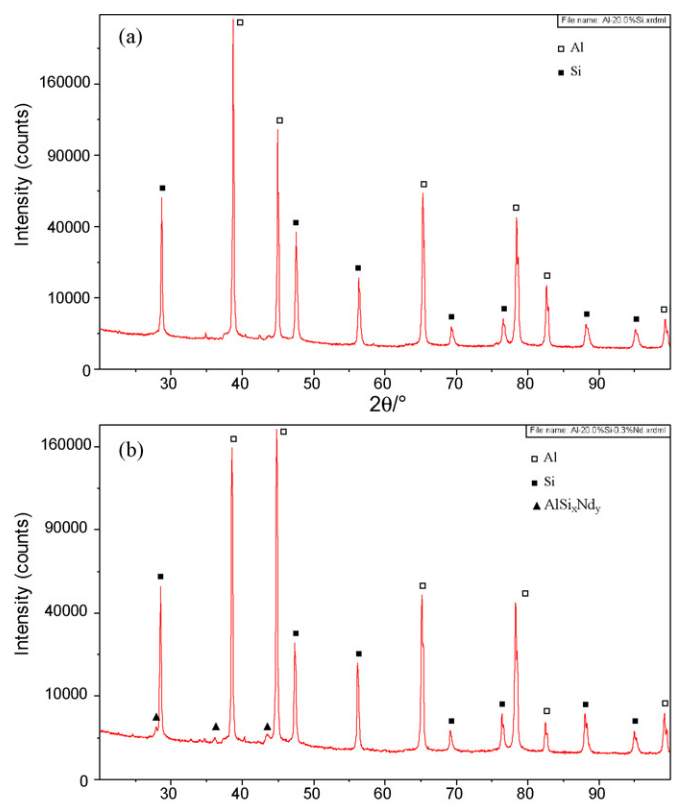

Fig. 6. XRD patterns of Al–20%Si before and after modification. (a) Unmodified sample and (b) modified sample.

Table 3
Composition of needle shape phase.

Element	Weight (%)	Atomic (%)
Al	36.5	64.1
Si	11.1	18.7
Nd	52.4	17.2

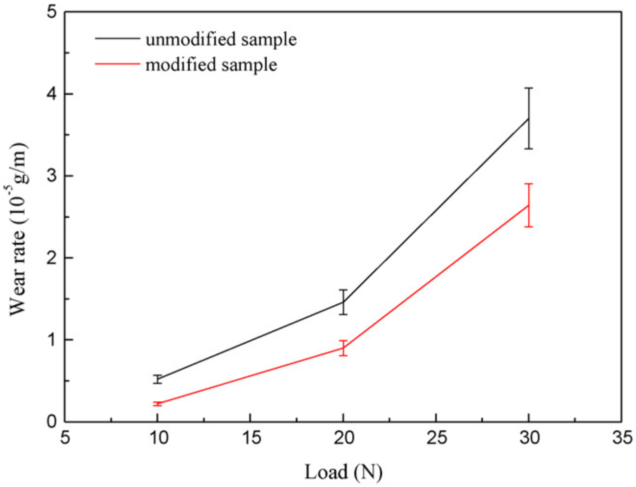

Fig. 7. The variation of wear rate of Al–20%Si alloy before and after modification with different loads.

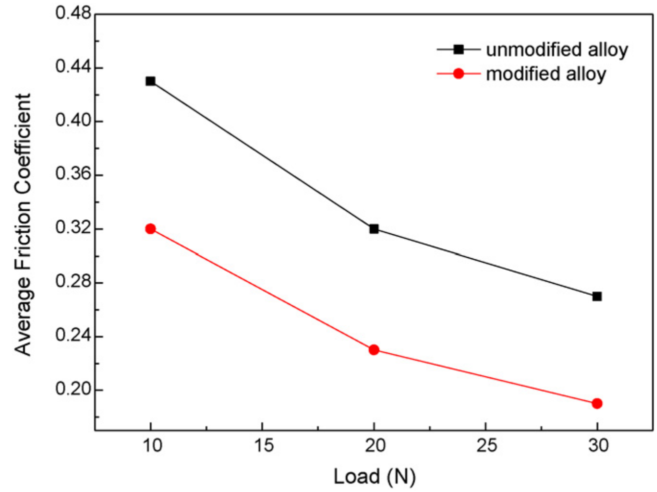

Fig. 8. The variation of friction coefficient of Al–20%Si alloy before and after modification with different loads.

or lamellar of initial sample to dot-like of modified sample. This indicates that Nd could also modify eutectic silicon.

Fig. 4 shows the TEM image and SAD pattern of Al–20%Si–0.3%Nd alloys. Fig. 4(a) gives microstructure of Al–20%Si–0.3%Nd alloy, it can be seen that a new needle shape phase forms on the boundary of Al and Si phases of modified sample. Fig. 4(b) presents SAD pattern of the phase, by calculating, d value of three different lattice plane is *d*(R1), *d*(R2) and *d*(R3), respectively, and they are much higher than that of (1 0 0) lattice plane of Al and Si phases. In order to analyze chemical composition the new phase. EDS analysis was

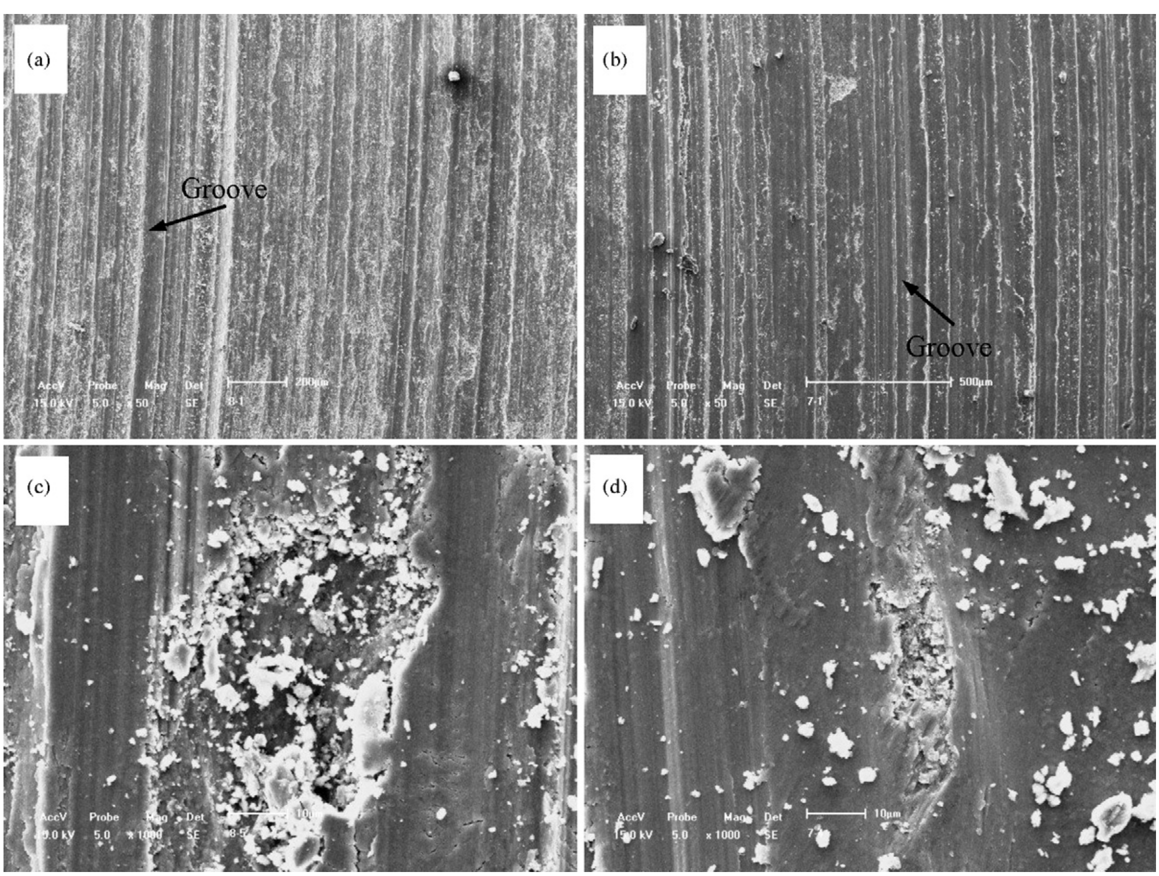

Fig. 9. SEM morphology of worn surface of Al–20%Si alloy before and after modification. (a) Al–20%Si alloy, (b) Al–20%Si–0.3%Nd alloy, (c) magnified picture of local area in (a), and (d) magnified picture of local area in (b).

carried out on the phase and results are shown in Fig. 5 and Table 3. The chemical composition of the phase is composed of Al (64.1 at.%), Si (18.7 at.%) and Nd (17.2 at.%). The results show that the Al–Si–Nd ternary phase is a Nd-rich phase and little reference has reported about crystal structure of the phase in the past.

Fig. 6(a) and (b) are the XRD patterns of Al–20%Si before and after modification. It can be seen that three little extra peaks emerges after modification [25]. However, the three peaks are not identical to any of the peaks of Al–Nd or Al–Si or Si–Nd binary phases. The *d* values of extra three peaks with low intensity are calculated by Bragg's equation. One of *d* values of three unidentified peaks is identical to *d*(R3). So, it can be deduced that these peaks should be diffraction peaks of the new phase found in TEM bright field image. The crystal structure and lattice mode will be investigated in detail in the future work.

3.2. Friction and wear

Smaller wear rate means higher wear resistance. Wear resistance of Al–Si alloy mainly depends on content of Si element, eutectic and primary Si morphology and distribution [26]. It is believed that higher Si content, fine and granular primary Si could improve the wear resistance of hypereutectic Al–Si alloys [21,27–29]. It has been reported the wear resistance of Al–Si alloys can be improved by grain refinement [30,31]. In this paper, wear rate was adopted to evaluate the wear resistance of Al–20Si alloy before and after modification.

In order to investigate the change of wear resistance before and after 0.3 wt.%Nd modification, wear rates of hypereutectic Al–20%Si alloys before and after modification were tested and the results are shown in Fig. 7. Fig. 7 indicates that the wear rates of the Al–20%Si alloys increased as a function of the loads. Furthermore, it can be clearly observed that the wear rates of the modified Al–20%Si alloy is lower than those of the unmodified Al–20%Si alloy (under loads ranging from 10 N to 30 N),the result is in agreement with research results of Jiang et al. [32] and Xu et al. [33]. The improvement in wear resistance is mainly due to the refinement of primary silicon [34] and the intermetallic compounds strengthen of ternary phase $AlSi_xNd_y$ [35,36]. So, the wear rates of modified Al–20%Si alloy significantly decreases compared with that of unmodified Al–20%Si alloy.

In order to study friction behavior of Al–20%Si alloy before and after Nd modification. Friction coefficients of Al–20%Si before and after modification with different loads during dry sliding process were measured and the results are shown in Fig. 8. In general, the friction coefficient is also an indicator of abrasion resistance. As can be seen in Fig. 8, friction coefficients of modified alloy are lower than that of initial samples for all the loads. Meantime, it can be found that the friction coefficient decreases with load increasing in 10–30 N range for all the samples. Such a reduction in friction coefficient may be associated with the formation of oxide layers during wear process as load increased [26]. The decrease in friction coefficient can be attributed to the development of oxide layers on the alloys [37], protecting the alloys from further severe surface damage and lowering the weight loss.

Fig. 9(a)–(d) show that SEM micrographs of worn surfaces of the unmodified and modified Al–20%Si alloys under 10 N load. Previous studies have revealed that the wear behavior of Al–Si alloys can be correlated to their microstructure features very well [38–40]. Thus, the morphologies and sizes of primary silicon in hypereutectic Al–Si alloys play a critical role in determining wear behavior of hypereutectic Al–Si alloys. Fig. 9(a) shows that broad and deep grooves form and a mass of debris appears on worn surface of unmodified Al–20%Si alloy. Fig. 9(b) shows that worn surface morphology of modified Al–20%Si alloy. Compared with that of unmodified Al–20%Si alloy, grooves becomes thinner and debris becomes fewer. Fig. 9(c) and (d) are magnified pictures of local area in Fig. 9(a) and (b), respectively. Fig. 9(c) shows that big wear pit forms on the worn surface of unmodified Al–20%Si alloy after wear test. Coarse primary silicon phase in unmodified Al–20%Si alloy could not be effectively bound by the matrix. So it fractured and partly peeled during worn test [32]. As a result, the wear resistance of unmodified Al–20%Si alloy decreased. Comparing modified Al–20%Si alloy (Fig. 9(d)) with unmodified Al–20%Si alloy (Fig. 9(c)), it can be observed that smaller wear pit appears on the worn surface of modified Al–20%Si alloy. Primary silicon phase is finer and strongly bound by the matrix in its position to resist the destructive action. As a result, the wear rate of the modified Al–20%Si alloy is lower than that of the unmodified Al–20%Si alloy.

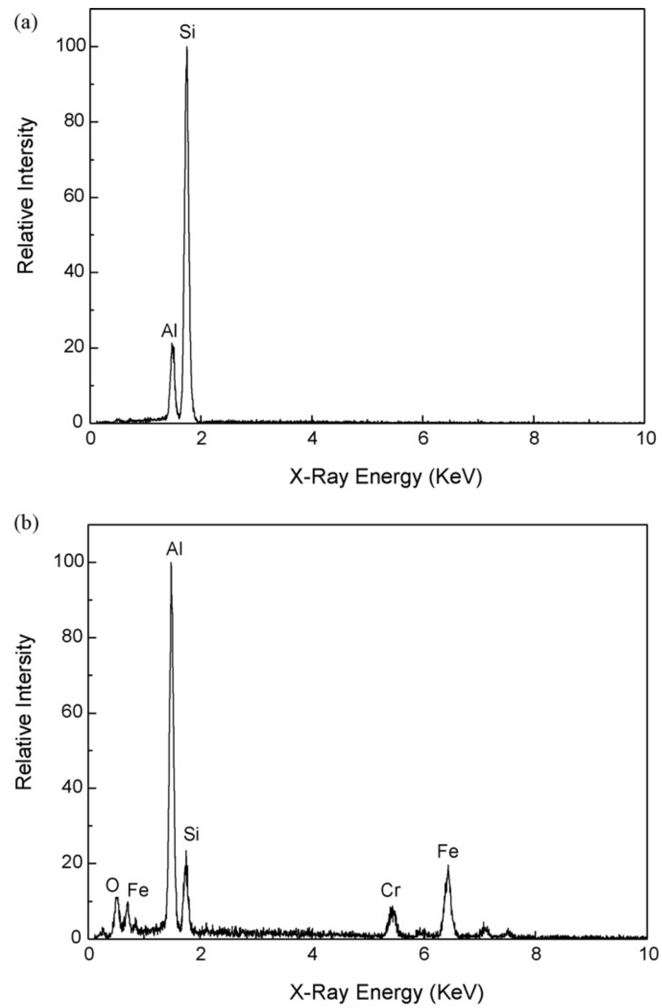

Fig. 10. EDS composition analysis of different positions in worn surface of alloy samples. (a) Unmodified sample and (b) modified sample.

Fig. 10(a) and (b) show EDS composition analysis results of different positions (Fig. 9(c) and (d)) of worn surfaces of initial and modified samples, respectively. Fig. 10(a) gives the composition analysis of worn surface of the Al–20%Si alloy and its main component is Si element. So, from the wear morphology and EDS analysis of wear zero, it can be concluded that wear mode of initial sample is mainly abrasive wear and adhesive wear. Fig. 10(b) gives the composition analysis of the wear surface of modified alloy. There are Fe, Cr, O and other elements on the wear surface. It proves that the material has transferred during the wear process and Fe, Cr abrasive elements in stainless steel counterparts were transferred to the internal pits, which indicates abrasive wear, adhesive wear and oxidative wear.

The wear mechanism for the Al–20%Si and Al–20%Si–0.3%Nd alloys was different from analysis of the worn surface. For Al–20%Si alloy, the abrasive wear and adhesive wear are the major wear mechanisms. Fracture of coarse Si phase occurred during wear process. Broad grooves and a mass of debris formed on the worn surface. Some large wear pits can be observed on the worn surface. In the case of Al–20%Si–0.3%Nd alloy, finer grooves and less debris formed on worn surface. Some small wear pits can be observed on the worn surface. EDS analyses show the worn surface of the pins contains a certain amount of Fe and O elements. This indicates that the abrasive wear, adhesive wear and oxidative wear mechanism operates during the wear test, the wear proceeds mainly by the formation of oxidative layer on the worn surface and its spalling [41,42]. Thus, abrasive wear, adhesive wear and oxidative wear is the dominant wear mechanism, the results are in agreement with Refs. [26,43].

4. Conclusions

OM, SEM analysis and wear tests show that 0.3 wt.%Nd could refine primary silicon and eutectic silicon of Al–20%Si alloy, change morphology of primary silicon and improve wear resistance of the alloy. The main conclusions can be summarized as follows:

a. The grain size of primary silicon is decreased from 80–120 μm to 20–50 μm, and the morphology changes from star to fine polyhedral. Eutectic silicon changed from acicular or lamellar morphology to dot-like morphology.
b. TEM results show that a new needle shape ternary phase ($AlSi_xNd_y$) forms in modified alloy.
c. XRD results show that three little unknown diffraction peaks appear after Nd modification and it is induced that they should be diffraction peaks of ternary $AlSi_xNd_y$ intermetallic phase in the modified alloy by analyzing both TEM and XRD results.
d. After 0.3 wt.%Nd modification, wear resistance of modified sample is significantly improved as compared to initial sample.
e. The dominant wear mechanism for Al–20%Si–0.3%Nd alloy is abrasive wear, adhesive wear and oxidative wear mechanism, and that for Al–20%Si alloy is abrasive wear and adhesive wear mechanism.

Acknowledgements

The present work is supported by Doctoral Fund of Ministry of Education of China (No. 200801451082) and National “Eleventh Five-Year” scientific and technological support to plan projects (2009BAE80B01).

References

[1] Y.P. Wu, S.J. Wang, H. Li, X.F. Liu, J. Alloys Compd. 477 (2009) 139–144.
[2] C.L. Xu, Q.C. Jiang, Y.F. Yang, H.Y. Wang, J.G. Wang, J. Alloys Compd. 422 (2006) L1–L4.
[3] S. Anand, T.S. Srivatsan, Y. Wu, E.J. Lavemia, J. Mater. Sci. 32 (1997) 2835–2848.
[4] J. Guo, Y. Liu, P.X. Fan, H.X. Qu, T. Quan, J. Alloys Compd. 477 (2010) 45–49.
[5] M. Zuo, K. Jiang, X.F. Liu, J. Alloys Compd. 503 (2010) L26–L30.
[6] H.S. Dai, X.F. Liu, Mater. Charact. 59 (2008) 1559–1563.
[7] C.M. Chen, C.C. Yang, C.G. Chao, J. Mater. Process. Technol. 167 (2005) 103–109.
[8] K. Matsuura, M. Kudoh, H. Kinoshita, H. Takahashi, Mater. Chem. Phys. 81 (2003) 393–395.
[9] B. Yang, F. Wang, J.S. Zhang, Acta Mater. 51 (2003) 4977–4989.
[10] J.Y. Qin, M. Zuo, T.K. Gu, X.F. Liu, J. Alloys Compd. 492 (2010) 525–528.
[11] M. Gupta, S. Ling, J. Alloys Compd. 287 (1999) 284–294.
[12] D.H. Lu, Y.H. Jiang, G.S. Guan, R.F. Zhou, Z.H. Li, R. Zhou, J. Mater. Process. Technol. 189 (2007) 13–18.
[13] F. Wang, B. Yang, X.J. Duan, B.Q. Xiong, J.S. Zhang, J. Mater. Process. Technol. 137 (2003) 191–194.
[14] H.K. Yi, D. Zhang, T. Sakata, H. Mori, J. Alloys Compd. 354 (2003) 159–164.
[15] B. Gao, L. Chen, F.X. Yu, S.C. Sun, G.F. Tu, Rare Met. 26 (6) (2007) 578–583.
[16] H.H. Zhang, H.L. Duan, G.J. Shao, L.P. Xu, Rare Met. 27 (1) (2008) 59–63.
[17] R. Sterner Rainer, US Patent 1940922, 26 December, 1933.
[18] D.K. Li, M. Zuo, Q. Zhang, X.F. Liu, J. Alloys Compd. 502 (2010) 304–309.
[19] J.Y. Chang, I.G. Moon, C.S. Choi, J. Mater. Sci. 33 (1988) 5015–5023.
[20] H.K. Yi, D. Zhang, Mater. Lett. 57 (2003) 2523–2529.
[21] S.A. Kori, T.M. Chandrashekharaiah, Wear 263 (2007) 745–755.
[22] D.K. Dwivedi, Mater. Des. 27 (2006) 610–616.
[23] B. Gao, L. Chen, S.C. Sun, G.F. Tu, X.M. Tian, T.J. Zhao, W.Y. Wu, X. Bian, J. Rare Earths 25 (2007) 473–476 (Special issue).
[24] F. Wang, Y.J. Ma, Z.Y. Zhang, X.H. Cui, Y.S. Jin, Wear 256 (2004) 342–345.
[25] D. Zhang, H.K. Yi, W.J. Li, T.X. Fan, Trans. Nonferrous Met. Soc. China 13 (3) (2003) 541–545.
[26] A.S. Anasyda, A.R. Daud, M.J. Ghazali, Mater. Des. 31 (2010) 365–374.
[27] M.D. Sexton, T.E. Fischer, Wear 96 (1984) 17–30.
[28] A.M. Zhao, W.M. Mao, Z.S. Zhen, C.M. Jiang, X.Y. Zhong, Trans. Nonferrous Met. Soc. China 11 (5) (2001) 827–833.
[29] R. Shivanath, P.K. Sengupta, T.S. Eyre, Br. Foundrymen 79 (1977) 349–356.
[30] A.K. Prasada Rao, K. Das, B.S. Murty, M. Chakraborty, Wear 257 (2004) 148–153.
[31] D.K. Dwivedi, Mater. Sci. Eng. A 382 (2004) 328–334.
[32] Q.C. Jiang, C.L. Xu, M. Lu, H.Y. Wang, Mater. Lett. 59 (2005) 624–628.
[33] Y. Xu, L.G. Lu, J. Bai, J. Rare Earths 25 (Suppl.) (2007) 94–97.
[34] A.K. Prasada Rao, K. Das, B.S. Murty, M. Chakraborty, Wear 261 (2006) 133–139.
[35] A. Wu, C. Xia, S. Wang, Rare Met. 25 (2006) 371–376.
[36] S. Radhakrishnan, G. Subbarayan, L. Nguyen, W. Mazotti, Mater. Des. 28 (2007) 2712–2718.
[37] K. Razavizadeh, T.S. Eyre, Wear 79 (1982) 325–333.
[38] B.K. Prasad, K. Venkateswarlu, O.P. Modi, A.H. Yegneswaran, J. Mater. Sci. Lett. 15 (1996) 1773–1776.
[39] S. Das, S.V. Prasad, T.R. Ramachandran, Wear 133 (1989) 173–187.
[40] S. Das, S.V. Prasad, T.R. Ramachandran, Mater. Sci. Eng. A 138 (1991) 123–132.
[41] R.D. Ott, C.A. Blue, M.L. Santella, P.J. Blau, Wear 251 (2001) 868–874.
[42] N. Saheb, T. Laoui, A.R. Daud, M. Harun, S. Radiman, R. Yahay, Wear 249 (2001) 656–662.
[43] T.M. Chandrashekharaiah, S.A. Kori, Tribol. Int. 42 (2009) 59–65.